# Mechanism of $Mg^{2+}$ Binding in the $Na^+,K^+$-ATPase

Anne Pilotelle-Bunner,[†‡] Flemming Cornelius,[§] Pierre Sebban,[‡] Philip W. Kuchel,[¶] and Ronald J. Clarke[†*]
[†]School of Chemistry, University of Sydney, Sydney, New South Wales, Australia; [‡]Laboratoire de Chimie-Physique, Université Paris-Sud/CNRS, Orsay, France; [§]Department of Physiology and Biophysics, University of Aarhus, Aarhus, Denmark; and [¶]School of Molecular and Microbial Biosciences, University of Sydney, Sydney, New South Wales, Australia

ABSTRACT The $Mg^{2+}$ dependence of the kinetics of the phosphorylation and conformational changes of $Na^+,K^+$-ATPase was investigated via the stopped-flow technique using the fluorescent label RH421. The enzyme was preequilibrated in buffer containing 130 mM NaCl to stabilize the E1$(Na^+)_3$ state. On mixing with ATP, a fluorescence increase was observed. Two exponential functions were necessary to fit the data. Both phases displayed an increase in their observed rate constants with increasing $Mg^{2+}$ to saturating values of 195 (± 6) $s^{-1}$ and 54 (± 8) $s^{-1}$ for the fast and slow phases, respectively. The fast phase was attributed to enzyme conversion into the E2MgP state. The slow phase was attributed to relaxation of the dephosphorylation/rephosphorylation (by ATP) equilibrium and the buildup of some enzyme in the E2Mg state. Taking into account competition from free ATP, the dissociation constant ($K_d$) of $Mg^{2+}$ interaction with the E1ATP$(Na^+)_3$ state was estimated as 0.069 (± 0.010) mM. This is virtually identical to the estimated value of the $K_d$ of $Mg^{2+}$-ATP interaction in solution. Within the enzyme-ATP-$Mg^{2+}$ complex, the actual $K_d$ for $Mg^{2+}$ binding can be attributed primarily to complexation by ATP itself, with no apparent contribution from coordination by residues of the enzyme environment in the E1 conformation.

## INTRODUCTION

An important role of $Mg^{2+}$ in biology is as a cofactor of ATP. The $Mg^{2+}$ ion is complexed by the negatively charged oxygens of its phosphate groups. The $Mg^{2+}$ is thus thought to help shield the negative charges of the phosphates, allowing reaction with the electron pairs of attacking groups and facilitating phosphoryl transfer (1). One of the most important enzymes in which this is the case is the $Na^+,K^+$-ATPase, which is responsible for maintaining electrochemical potential gradients for $Na^+$ and $K^+$ across the plasma membrane.

To our knowledge, no crystal structure of the $Na^+,K^+$-ATPase in the E1 state with bound $Mg^{2+}$ and ATP has yet been reported. Nevertheless, based on a published crystal structure of the related enzyme sarcoplasmic reticulum $Ca^{2+}$-ATPase (2), and using computer modeling, Patchornik et al. (3) suggested that, like the phosphates of ATP, the aspartate residues D710, D443, and D714 contribute to $Mg^{2+}$ coordination. Although this may be correct, it is difficult from crystal structural data to make conclusions about the relative strengths of interactions. The aim of this article is to provide reliable experimental data on the strength of binding of $Mg^{2+}$ ions to the $Na^+,K^+$-ATPase.

A difficulty in studying $Mg^{2+}$ interaction with the $Na^+,K^+$-ATPase under physiological conditions, i.e., in the presence of ATP and $Na^+$ ions, is that it immediately induces phosphorylation, so that $Mg^{2+}$ binding cannot be separated from the phosphorylation reaction. This precludes equilibrium binding studies. Here we have, therefore, applied a pre-steady-state kinetic technique (stopped-flow spectrofluorimetry) utilizing the voltage-sensitive fluorescent probe RH421. Together with data recently obtained under the same experimental conditions for $Mg^{2+}$ binding to ATP (4), this allows us to analyze the question of the relative contributions of the enzyme and ATP in binding $Mg^{2+}$ in the enzyme-ATP-$Mg^{2+}$ complex. In the case of the E1 conformation of the enzyme, it will be shown here that, although the enzyme environment is definitely important for the catalysis of phosphoryl transfer from ATP, coordination by ATP dominates the dissociation constant ($K_d$) for $Mg^{2+}$ binding.

## MATERIALS AND METHODS

### Enzyme and reagents

$Na^+,K^+$-ATPase-containing membrane fragments from shark rectal glands were purified essentially as described by Skou and Esmann (5). The specific ATPase activity at 37°C and pH 7.4 was measured according to the methods of Ottolenghi (6). The activity of the preparation used was 1679 $\mu$mol ATP hydrolyzed $h^{-1}$ (mg of protein)$^{-1}$ and the protein concentration was 4.82 mg $mL^{-1}$. The protein concentration was determined according to the Peterson modification (7) of the Lowry method (8) using bovine serum albumin as a standard. For the calculation of the molar protein concentration, a molecular mass for an $\alpha\beta$ unit of the $Na^+,K^+$-ATPase of 147,000 g $mol^{-1}$ (9) was used. The origins of the various reagents used were imidazole (≥99%, Sigma, Castle Hill, Australia), NaCl (suprapure, Merck, Kilsyth, Australia), $MgCl_2$ $6H_2O$ (analytical grade, Merck), EDTA (99%, Sigma), ATP disodium $3H_2O$ (≥99%, Sigma) and HCl (0.1 N Titrisol solution, Merck).

### Stopped-flow spectrofluorimetry

Stopped-flow experiments were carried out using an SF-61 stopped-flow spectrofluorimeter from Hi-Tech Scientific (Salisbury, United Kingdom) as described previously (10). To improve the signal/noise ratio, typically 20–30 experimental traces were averaged before the $k_{obs}$ values were

*Submitted December 4, 2008, and accepted for publication January 28, 2009.*

*Correspondence: r.clarke@chem.usyd.edu.au

Editor: Edward H. Egelman.



0006-3495/09/05/3753/9 $2.00

doi: 10.1016/j.bpj.2009.01.042

evaluated. This was done by fitting a sum of two exponential functions to the averaged experimental trace. The kinetics of the $Na^+$,$K^+$-ATPase conformational changes and ion translocation reactions were investigated at 24°C in the stopped-flow apparatus by mixing $Na^+$,$K^+$-ATPase (labeled with RH421) with an equal volume of a 2-mM ATP solution. Both solutions were prepared in a buffer containing 30 mM imidazole, 130 mM NaCl, and varying concentrations of $MgCl_2$. No change in the $Na^+$ or $Mg^{2+}$ concentration occurred on mixing.

## Data fitting

Nonlinear least-squares fitting of equations describing the $Mg^{2+}$ dependence of the fluorescence amplitudes to the data was performed using Origin 6.0 (Microcal Software, Northampton, MA). Fitting of equations describing the $Mg^{2+}$ dependence of the $k_{obs}$ values to the data were performed using Mathematica (version 6.0.2, Wolfram Research, Champaign, IL) via a globally convergent variation of the Newton-Raphson methods to find the roots of Eqs. 1 and 2.

Immediately after mixing with ATP, but before any phosphorylation, the following equilibria would be expected to exist in solution:

$$\mathrm{E1ATP}\left(\mathrm{Na}^+\right)_3 + \mathrm{Mg}^{2+} \leftrightarrow \mathrm{E1MgATP}\left(\mathrm{Na}^+\right)_3$$

$$\mathrm{ATP} \quad + \quad \mathrm{Mg}^{2+} \leftrightarrow \mathrm{MgATP}.$$

$K_E$ and $K_{ATP}$ are the association constants for each equilibrium. We assume that because the enzyme is saturated by ATP and $Na^+$ there is no enzyme in the E1$(Na^+)_3$, E1ATP, or E1 states, and therefore, binding of $Mg^{2+}$ to these states has been ignored. We also assume that under conditions of excess ATP and $Mg^{2+}$ over enzyme, the concentrations of E1MgATP$(Na^+)_3$ and E1ATP$(Na^+)_3$ can be neglected when calculating the total ATP concentration and that the concentration of E1MgATP$(Na^+)_3$ can also be neglected when calculating the total $Mg^{2+}$ concentration. Under these conditions, taking into account mass balance for ATP, the free ATP concentration is related to the total $Mg^{2+}$ concentration ($[Mg^{2+}]_{tot}$) and the total ATP concentration ($[ATP]_{tot}$) by

$$[\mathrm{ATP}] + \frac{K_{\mathrm{ATP}}[\mathrm{ATP}]\left[\mathrm{Mg}^{2+}\right]_{\mathrm{tot}}}{1 + K_{\mathrm{ATP}}[\mathrm{ATP}]} - [\mathrm{ATP}]_{\mathrm{tot}} = 0. \quad (1)$$

Solving for the roots of Eq. 1 allows [ATP] to be calculated for any values of $[Mg^{2+}]_{tot}$ and $[ATP]_{tot}$. Considering mass balance for $Mg^{2+}$, the free $Mg^{2+}$ concentration is related to the $[Mg^{2+}]_{tot}$ and the total enzyme concentration ($[E]_{tot}$) by

$$\left[\mathrm{Mg}^{2+}\right] + K_{\mathrm{ATP}}[\mathrm{ATP}]\left[\mathrm{Mg}^{2+}\right] + \frac{K_{\mathrm{E}}[\mathrm{E}]_{\mathrm{tot}}\left[\mathrm{Mg}^{2+}\right]}{1 + K_{\mathrm{E}}\left[\mathrm{Mg}^{2+}\right]} - \left[\mathrm{Mg}^{2+}\right]_{\mathrm{tot}} = 0. \quad (2)$$

Once Eq. 1 has been solved for [ATP], this can be used to solve for the roots of Eq. 2 to find $[Mg^{2+}]$ for any values of $[Mg^{2+}]_{tot}$ and $[E]_{tot}$. Taking into account mass balance for the enzyme, from the expression for the association constant of $Mg^{2+}$ with the enzyme, the concentration of E1MgATP$(Na^+)_3$, the species which must be produced to allow phosphorylation to occur, is

$$\left[\mathrm{E1MgATP}\left(\mathrm{Na}^+\right)_3\right] = \frac{K_{\mathrm{E}}[\mathrm{E}]_{\mathrm{tot}}\left[\mathrm{Mg}^{2+}\right]}{1 + K_{\mathrm{E}}\left[\mathrm{Mg}^{2+}\right]}. \quad (3)$$

The degree of saturation ($S_{E1}$) of the $Mg^{2+}$ sites on the E1 conformation of the enzyme is given by

$$S_{\mathrm{E1}} = \frac{\left[\mathrm{E1MgATP}\left(\mathrm{Na}^+\right)_3\right]}{[\mathrm{E}]_{\mathrm{tot}}}. \quad (4)$$

After the enzyme has been mixed with ATP and cycling has begun, $Mg^{2+}$ could also bind to the E2 conformation of the enzyme according to the equilibrium

$$\mathrm{E2ATP} + \mathrm{Mg}^{2+} \leftrightarrow \mathrm{E2MgATP}.$$

$K_F$ represents the association constant for this equilibrium. Taking an approach similar to that taken for the E1 conformation, one can find the free $Mg^{2+}$ concentration when the enzyme is in the E2 conformation by solving an expression analogous to Eq. 2, i.e.,

$$\left[\mathrm{Mg}^{2+}\right] + K_{\mathrm{ATP}}[\mathrm{ATP}]\left[\mathrm{Mg}^{2+}\right] + \frac{K_F[\mathrm{E}]_{\mathrm{tot}}\left[\mathrm{Mg}^{2+}\right]}{1 + K_F\left[\mathrm{Mg}^{2+}\right]} - \left[\mathrm{Mg}^{2+}\right]_{\mathrm{tot}} = 0. \quad (5)$$

Equation 1 can still be used to calculate the free ATP concentration. The degree of saturation ($S_{E2}$) of the $Mg^{2+}$ sites on the enzyme is given by

$$S_{\mathrm{E2}} = \frac{K_F\left[\mathrm{Mg}^{2+}\right]}{1 + K_F\left[\mathrm{Mg}^{2+}\right]}. \quad (6)$$

# RESULTS

## Rates of ATP-induced stopped-flow fluorescence traces

On mixing $Na^+$,$K^+$-ATPase-containing membrane fragments labeled with RH421 with $Na_2ATP$ (as described under Materials and Methods), an increase in fluorescence occurred (see Fig. 1). Two exponential time functions were required to fit the data. The faster phase constituted on average 80% of the overall amplitude and the slower phase 20%. As the $MgCl_2$ concentration of the enzyme suspension and the ATP solution was increased, the overall kinetics of the fluorescence change became faster until a saturating limit was reached with an observed rate constant, $k_{obs}$, of ~190–200 $s^{-1}$ for the faster phase (see Fig. 2) and ~45–50 $s^{-1}$ for the slower phase (see Fig. 3). These data agree qualitatively with previous measurements using the same source of enzyme (11). The $k_{obs}$ values measured agree quantitatively with similar measurements on enzyme from rabbit and pig kidney (10,12). The fact that the kinetics of both phases saturate at constant values implies that the overall rate-determining step for each process is a first-order reaction (i.e., phosphorylation or an enzyme conformational change). The slower kinetics observed under nonsaturating $Mg^{2+}$ concentrations implies that both first-order reactions are preceded by $Mg^{2+}$ binding.

A control experiment in which 5 mM EDTA and no $MgCl_2$ were included in the buffer resulted in almost complete disappearance of the fluorescence change (see Fig. 1). In previous studies (10), it was shown that if the $Na^+$,$K^+$-ATPase membrane fragments were preequilibrated with 30 mM vanadate, subsequent mixing with ATP caused no fluorescence change. These control experiments indicate that the observed fluorescence changes are due to the hydrolytic action of the $Na^+$,$K^+$-ATPase.

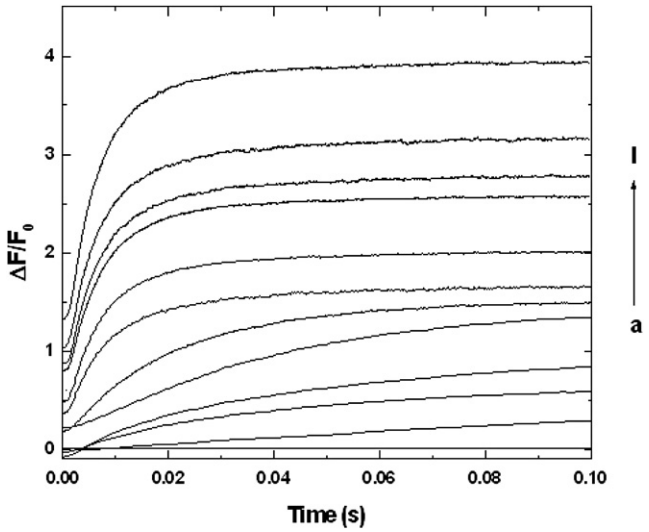


FIGURE 1 Stopped-flow fluorescence transients of $Na^+,K^+$-ATPase noncovalently labeled with RH421 (100 nM after mixing). $Na^+,K^+$-ATPase (270 nM after mixing) was rapidly mixed with an equal volume of $Na_2ATP$ solution (1 mM after mixing). Each solution was in buffer containing 130 mM NaCl, 30 mM imidazole, and either 5 mM EDTA or varying concentrations of $MgCl_2$ (pH 7.4, 24°C). The traces have been labeled in order of increasing fluorescence intensity change or, equivalently, increasing final fluorescence level, i.e., curve *a* has the lowest and curve l the highest final fluorescence intensity. Curve *a* is a control experiment in the presence of 5 mM EDTA and no added $MgCl_2$. Curves *b–l* correspond to the $MgCl_2$ concentrations 0.0025 mM, 0.01 mM, 0.15 mM, 0.2 mM, 0.4 mM, 1.0 mM, 2.0 mM, 2.5 mM, 3.5 mM, 4.5 mM, and 5.0 mM, respectively. The excitation and emission wavelengths were 577 nm and ≥665 nm (RG665 glass cutoff filter), respectively.

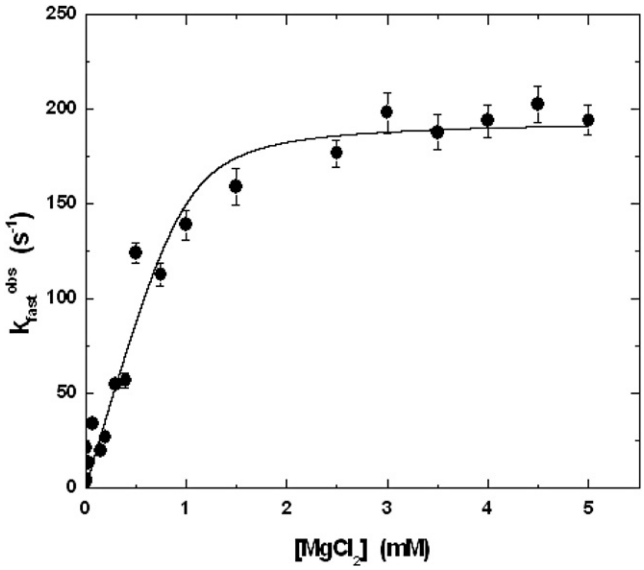


FIGURE 2 Dependence of the observed rate constant of the fast phase ($k_{fast}^{obs}$) of the RH421 fluorescence change on the concentration of $MgCl_2$ (after mixing). The solid line is a nonlinear least-squares fit of the data to Eq. 8 and Eqs. 1–4. The fit parameters were $k_1 = 195\ (\pm\ 6)\ s^{-1}$ and $K_E = 1.45\ (\pm\ 0.22) \times 10^4\ M^{-1}$. $K_E$ corresponds to a $K_d$ of 0.069 (± 0.010) mM.

Based on previous studies (11,13,14), it is known that RH421 responds to the formation of the E2P state with an increase in fluorescence. The fast phase of the fluorescence transients observed can therefore confidently be attributed to the reaction $E1MgATP(Na^+)_3 \rightarrow E2MgP + 3Na^+ +$ ADP. The maximum $k_{obs}$ for the fast phase (195 $s^{-1}$) agrees with $k_{obs}$ values determined for enzyme phosphorylation using the quenched-flow technique and radioactively labeled ATP, which yield values of the order of 200 $s^{-1}$ (10,15,16). Phosphorylation can thus be considered as the rate-determining step for the reaction sequence responsible for the fast fluorescence phase under these experimental conditions. At lower temperatures, i.e., ≤15°C, a difference in the kinetics observed via stopped-flow using RH421 and quenched flow is apparent (11), indicating that as the temperature decreases, the $E1MgP \rightarrow E2MgP$ transition makes an increasing contribution to the overall rate determination.

Based on additional stopped-flow measurements and theoretical simulations (12), the slow phase has previously been attributed to relaxation of the dephosphorylation/rephosphorylation equilibrium. The meaning of this requires some explanation. In the absence of $K^+$ ions, as in the experiments performed here, dephosphorylation of E2MgP is slow. Measured rate constants are in the range 2–7 $s^{-1}$ (17–20). After dephosphorylation, because excess ATP is present, the enzyme can undergo a conformational transition back to the E1 state and be rephosphorylated by ATP, i.e., $E2 \rightarrow E1(Na^+)_3 + ATP \rightarrow E2P + 3Na^+ +$ ADP ($Mg^{2+}$ ions have been omitted here for simplicity). The rate-

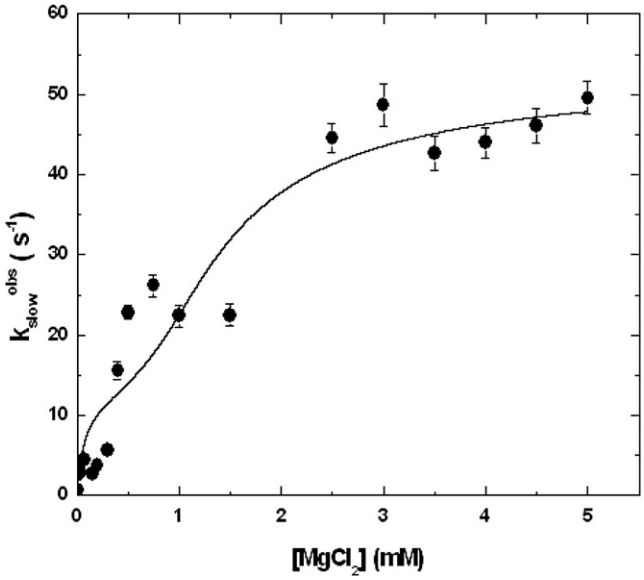


FIGURE 3 Dependence of the observed rate constant of the slow phase ($k_{slow}^{obs}$) of the RH421 fluorescence change on the concentration of $MgCl_2$ (after mixing). The solid line is a nonlinear least-squares fit of the data to Eq. 12 and Eqs. 1–6. The fit parameters were $k_4^{min} = 13(\pm 4)s^{-1}$, $k_4^{max} = 74(\pm 10)s^{-1}$, and $K_F = 1.3\ (\pm\ 0.8) \times 10^3\ M^{-1}$. $K_F$ corresponds to a $K_d$ of 0.8 (± 0.5) mM.

determining step in this rephosphorylation pathway is the conformational transition, E2 → E1($Na^+$)$_3$, which based on previous measurements would be expected to have a rate constant in the range 65–90 $s^{-1}$ (21–23) at saturating $Na^+$, $Mg^{2+}$, and ATP concentrations. Based on the Van Slyke approximation (24), the reciprocal of the overall expected rate constant for the entire pathway from E2 to E2P via ATP rephosphorylation is given by the sum of the reciprocals of the rate constants of the separate reaction steps, E2 → E1($Na^+$)$_3$ and E1($Na^+$)$_3$ + ATP → E2P + 3$Na^+$ + ADP. Taking values of 65–90 $s^{-1}$ for the first reaction, and the value of 195 $s^{-1}$ measured here for the fast phase for the second reaction, yields an overall expected rate constant in the range 49–62 $s^{-1}$.

Enzyme dephosphorylation and rephosphorylation via ATP represent a coupled equilibrium that must relax subsequent to the initial phosphorylation of the enzyme by ATP. The $k_{obs}$ value for the relaxation of any first or pseudo-first-order process is given by the sum of the forward and backward rate constants. Therefore, adding the rate constants given above for dephosphorylation and rephosphorylation yields an expected $k_{obs}$ of 51–69 $s^{-1}$. The $k_{obs}$ of 45–50 $s^{-1}$ measured here for the slow phase at a saturating $MgCl_2$ concentration is only slightly below this range. This small difference may perhaps be accounted for by the different enzyme sources (i.e., animal species) employed in the previous studies.

Further evidence supporting the assignment of the slow phase to the relaxation of the dephosphorylation/rephosphorylation equilibrium comes from measurements in which 7 mM KCl was included in the buffer before mixing with ATP (19). Under these conditions, an increase in fluorescence was still observed, but the fluorescent transient was then monoexponential. This can be explained by an acceleration of the dephosphorylation reaction by $K^+$ ions. The rate constant for $K^+$-stimulated dephosphorylation has been estimated based on stopped-flow measurements (19,25) to have a value of ~312 $s^{-1}$. Adding this value to the rate constant for rephosphorylation given above (49–62 $s^{-1}$), then yields an expected $k_{obs}$ for relaxation of the dephosphorylation/rephosphorylation equilibrium of 361–374 $s^{-1}$. This is far greater than the $k_{obs}$ found here for the fast phase due to initial ATP phosphorylation of 195 $s^{-1}$. Therefore, under $K^+$-saturating conditions, the dephosphorylation/rephosphorylation equilibrium would be expected to relax instantaneously on the timescale of the initial phosphorylation, which is consistent with the experimental observation of only a single phase under these conditions.

It has been suggested previously (11) that the slow phase could be due to a slower conformational change after formation of the E2P species, i.e., E2P → E2*P, where the E2*P phosphoenzyme form is a $K^+$-insensitive form in contrast to the $K^+$-sensitive E2P form. However, it has since been found that the model we present here is capable of explaining the ATP concentration dependence of both the $k_{obs}$ values and the amplitudes of the transients (21).

## Model simulations of the stopped-flow fluorescence transients

To gain a deeper understanding of the $Mg^{2+}$ dependence of the observed kinetic behavior, we have carried out simulations of the fluorescence transients based on the assignment of the fast and slow kinetic phases described above. Accordingly, the sequence of reaction steps used was

$$\mathrm{E1MgATP}\left(\mathrm{Na}^+\right)_3 \xrightarrow{k_1} \mathrm{E2MgP}\left(\mathrm{Na}^+\right)_3 + \mathrm{ADP} \qquad \text{(A)}$$

$$\mathrm{E2MgP}\left(\mathrm{Na}^+\right)_3 \underset{k_{-2}}{\overset{k_2}{\rightleftarrows}} \mathrm{E2MgP} + 3\mathrm{Na}^+ \qquad \text{(B)}$$

$$\mathrm{E2MgP} \underset{k_{-3}}{\overset{k_3}{\rightleftarrows}} \mathrm{E2Mg}. \qquad \text{(C)}$$

Mathematical details of the simulations are given in the Appendix. Remember that $k_{-3}$ represents the rate constant for rephosphorylation of the enzyme by continuing around the enzymatic cycle via E1 and undergoing phosphorylation by ATP; it is not the rate constant for ''back-door'' phosphorylation by inorganic phosphate. Reaction B describes the $Na^+$-binding equilibrium to the E2P state. Reaction A is required for the initial turnover of the enzyme after mixing with ATP. For subsequent turnovers, this reaction is incorporated in the reverse direction of reaction C.

Simulations based on this model (see Fig. 4) show that a biphasic fluorescence increase is expected as long as the fluorescence of dye associated with enzyme in the E2Mg state is greater than that of dye associated with the initial E1MgATP($Na^+$)$_3$ state. This agrees with the results of previous stopped-flow experiments showing that the fluorescence of RH421 decreases when the enzyme undergoes the transition from the E2 state to the E1($Na^+$)$_3$ state (10,12,26). In fact, as shown previously (12), a biphasic fluorescence increase would also be expected for a mechanism involving only reactions A and C. This would require the fluorescence level of the E2Mg state to be greater than that of the E2MgP state. However, since evidence exists (14,20,27) that fluorescence changes of RH421 associated with the $Na^+$,$K^+$-ATPase arise predominantly from steps involving ion binding to or release from the enzyme, we favor the complete reaction scheme A–C.

Based on the simulations, the observed two-phase fluorescence increase can be understood as follows. Initially, the enzyme is in the low fluorescent state, E1MgATP($Na^+$)$_3$. The fast phase of the fluorescence increase on mixing with ATP can be explained by phosphorylation of the enzyme and its conversion into the higher fluorescent state E2MgP. The slow phase of the fluorescence increase is attributed to the conversion of some of the enzyme into the other high fluorescent state, E2Mg.

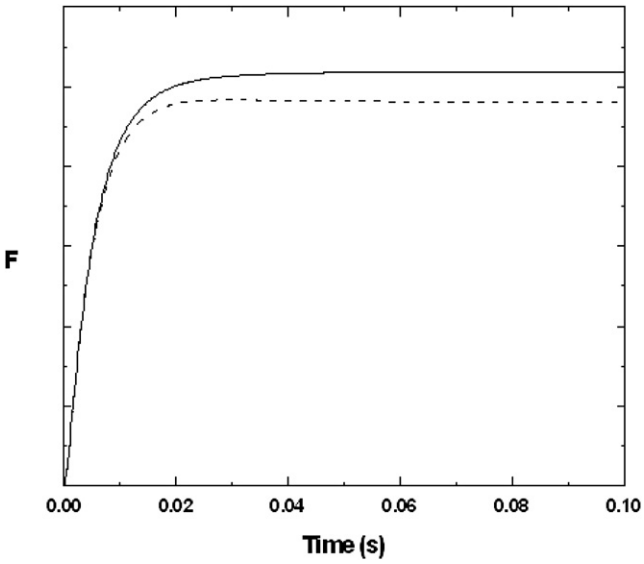


FIGURE 4 Computer simulations of RH421 stopped-flow kinetic transients for experiments in which $Na^+$,$K^+$-ATPase membrane fragments are mixed with ATP in the presence of $Mg^{2+}$. The simulations are based on reaction scheme A–C and have been calculated according to Eqs. A1–A5 (see Appendix). The values of the rate constants chosen for the simulations are $k_1 = 237\ s^{-1}$, $k_2 = k_{-2} = 1000\ s^{-1}$, $k_3 = 5\ s^{-1}$, and $k_{-3} = 63\ s^{-1}$. The solid line represents a simulation in which the fluorescence levels of the E2Mg and E2MgP states are assumed to be equal ($f_{E2Mg} = f_{E2MgP} = 1$) and the fluorescence level of the E1MgATP($Na^+$)$_3$ state is defined as zero ($f_{E1} = 0$). This simulation shows a biphasic fluorescence increase, as experimentally observed (cf. Fig. 1, *curve l*). The dashed line represents a simulation in which the fluorescence level of the E2Mg state is assumed to be less than that of the E2MgP state and equal to that of the E1MgATP($Na^+$)$_3$ state, i.e., $f_{E2MgP} = 1, f_{E2Mg} = f_{E1} = 0$. This simulation reaches a maximum in fluorescence intensity 0.3 s after mixing (not easily observable by eye), after which there is a slight drop in fluorescence. The time course of the dashed curve does not correspond to the experimentally observed behavior.

## Fitting of the fast phase of the stopped-flow kinetic data

Because phosphorylation of the enzyme by ATP also requires a $Mg^{2+}$ ion to bind as a cofactor, under conditions of excess $Na^+$, ATP, and $Mg^{2+}$ over enzyme, the initial formation of the E2MgP state can be considered as a pseudo-first-order reaction that requires complete saturation of the $Mg^{2+}$ binding sites to relax with its maximum rate constant. Under these conditions, it can be shown (10) that if one neglects competition between enzyme and unbound ATP for $Mg^{2+}$, the expected dependence of the observed rate constant for the fast phase ($k_{fast}^{obs}$) on the $Mg^{2+}$ concentration is given by

$$k_{fast}^{obs} = k_1 \times \frac{[Mg^{2+}]}{K_d + [Mg^{2+}]}, \quad (7)$$

where $k_1$ is the overall rate constant for phosphorylation of the enzyme and its conversion into the E2P state and $K_d$ is the apparent dissociation constant of $Mg^{2+}$ and enzyme in the E1ATP state. The term $[Mg^{2+}]/(K_d + [Mg^{2+}])$ represents the fraction of $Mg^{2+}$ sites of E1ATP occupied by $Mg^{2+}$. Equation 7 predicts a hyperbolic dependence of $k_{fast}^{obs}$ on the $Mg^{2+}$ concentration. However, in fact the situation is more complicated, because if the dissociation constants of ATP and enzyme for $Mg^{2+}$ are of a similar order of magnitude, excess unbound ATP would compete effectively with the enzyme for the available $Mg^{2+}$. This effect needs to be taken into account if one wishes to derive accurate values of $k_1$ and $K_d$.

Equation 7 can be written in a more model-independent form as

$$k_{fast}^{obs} = k_1 S_{E1}, \quad (8)$$

where $S_{E1}$ represents the degree of saturation of the $Mg^{2+}$ sites on the E1ATP($Na^+$)$_3$ species. Competition between enzyme and free ATP for $Mg^{2+}$ can be taken into account as described under Materials and Methods. Equations 1–4 allow one to calculate a value of $S_{E1}$ for any given values of the binding constants of enzyme and ATP for $Mg^{2+}$ and, in combination with Eq. 8, to fit this model to the experimental $k_{fast}^{obs}$ data. Following this procedure leads to values of $k_1$ and $K_d$ of 195 ($\pm$ 6) $s^{-1}$ and 0.069 ($\pm$ 0.010) mM, respectively. The value of $k_1$ agrees with measurements on enzyme from other sources under comparable conditions (10,12,21,22). The value of $K_d$ is indistinguishable from the dissociation constant of ATP alone for $Mg^{2+}$ (0.071 ($\pm$ 0.003) mM) under the same buffer conditions (4).

The salt concentrations are important here, because $Mg^{2+}$ can also interact with the $Na^+$ transport sites with an intrinsic $K_d$ of ~0.8 mM (28,29) and ATP can be complexed by $Na^+$ ions, both of which could make the apparent $K_d$ dependent on the NaCl concentration. In the absence of any other added ions, Grisham and Mildvan (30) reported that $Mg^{2+}$ binding to the enzyme in the absence of ATP and of added salt occurred with an apparent $K_d$ of 0.15 mM, whereas in a buffer containing 100 mM NaCl and 10 mM KCl, i.e., comparable to our conditions of 130 mM NaCl, the apparent $K_d$ was 1.0 mM. This value can't be directly compared to the $K_d$ determined here, though, because it is due to direct binding of $Mg^{2+}$ to the enzyme, whereas we are measuring the binding of $Mg^{2+}$ to an enzyme-ATP complex.

## Fitting of the slow phase of the stopped-flow kinetic data

In the case of the slow phase, attributed to the relaxation of reaction C above, under saturating conditions the observed rate constant should be given by the sum of the forward and backward rate constants:

$$k_{slow}^{obs} = k_3^{obs} + k_{-3}^{obs}. \quad (9)$$

The ''obs'' superscripts are used to indicate that under non-saturating conditions, these rate constants of reaction C could depend on the $Mg^{2+}$ concentration due to coupling to other reactions. In fact, the backward reaction of reaction C involves at least two steps:

$$\mathrm{E2Mg} \xrightarrow{k_4^{obs}} \mathrm{E1Mg(Na^+)_3}$$
$$\mathrm{E1Mg(Na^+)_3} + \mathrm{ATP} \xrightarrow{k_1^{obs}} \mathrm{E2P} + 3\mathrm{Na^+} + \mathrm{ADP}. \quad \text{(D)}$$

ATP and $Na^+$ binding reactions have not been explicitly included here, because we assume that these reactions are in fast equilibrium and that both ATP and $Na^+$ are present at saturating concentrations. Furthermore, we have neglected the reverse reaction of the conformational change of unphosphorylated enzyme ($E1Mg(Na^+)_3 \rightarrow E2Mg$), because in the absence of $K^+$ and the presence of high concentrations of both $Na^+$ and ATP, the E1/E2 equilibrium would be expected to lie greatly in favor of E1. According to the Van Slyke approximation (24) for sequential irreversible reactions, the overall observed rate constant for this reaction sequence can be approximated by

$$\frac{1}{k_{-3}^{obs}} = \frac{1}{k_4^{obs}} + \frac{1}{k_1^{obs}}, \quad (10)$$

where $k_1^{obs}$ is the same as the experimentally determined $k_{fast}^{obs}$. Therefore, after substituting from Eq. 8, rearranging and substituting the resulting expression for $k_{-3}^{obs}$ into Eq. 9 gives

$$k_{slow}^{obs} = k_3^{obs} + \frac{k_4^{obs} k_1 S_{E1}}{k_1 S + k_4^{obs}}. \quad (11)$$

This equation predicts an approximately hyperbolic increase in $k_{fast}^{obs}$ with increasing $Mg^{2+}$ as experimentally observed (see Fig. 3) with a saturating value given by $k_3^{obs} + (k_4^{obs} k_1/(k_1 + k_4^{obs}))$. The $Mg^{2+}$ dependence of $k_{fast}^{obs}$ could, thus, be explained by $Mg^{2+}$-stimulation of the phosphorylation reaction, as is the case for the fast phase. In the first instance, therefore, Eqs. 11 and 1-4 were fitted to the experimental $k_{slow}^{obs}$ data with the assumption that $k_3^{obs}$ and $k_4^{obs}$ are both independent of the $Mg^{2+}$ concentration. An adequate fit to the data could, however, only be achieved if $K_E$, the binding constant of $Mg^{2+}$ to $E1ATP(Na^+)_3$, was also allowed to vary. The best-fit value of $K_E$ was a factor of 10 lower than that already determined from the analysis of the fast phase (i.e., $K_d$ was a factor of 10 higher). Because this situation would be inconsistent, the possibility that $k_4^{obs}$ is also $Mg^{2+}$-dependent needs to be considered.

A $Mg^{2+}$ dependence of $k_4^{obs}$ could come about if $Mg^{2+}$ binding to E2 stimulates the E2 $\rightarrow$ E1 transition via an allosteric effect. This is already known to be the case for ATP (31). To consider such an effect, Eq. 11 must be modified to

$$k_{slow}^{obs} = k_3^{obs} + \frac{\left[k_4^{min} + \left(k_4^{max} - k_4^{min}\right) S_{E2}\right] k_1 S_{E1}}{k_1 S_{E1} + \left[k_4^{min} + \left(k_4^{max} - k_4^{min}\right) S_{E2}\right]}, \quad (12)$$

where $k_4^{min}$ and $k_4^{max}$ represent the minimum and maximum values of $k_4$ when the E2 state of the enzyme has no bound $Mg^{2+}$ ions and when it is saturated by $Mg^{2+}$, respectively. $S_{E1}$ and $S_{E2}$ represent the degrees of saturation of the E1 and E2 states by $Mg^{2+}$. $S_{E1}$ can be calculated by taking into account competition from the excess unbound ATP, according to Eqs. 1–6. Analogous equations can be written for the E2 state to allow the calculation of $S_{E2}$.

A fit of Eq. 12 to the experimental data is shown in Fig. 3. The fit was carried out using a fixed value of $K_{ATP}$, taken from calorimetric measurements (4), and fixed values of $k_1$ and $K_E$, based on the values determined from the analysis of the fast phase (see the previous section). The only parameters allowed to vary were $k_3^{obs}, k_4^{min}, k_4^{max}$ and $K_F$ (the binding constant of $Mg^{2+}$ to the E2ATP conformation of the protein). It was found that the value of $k_3^{obs}$, the rate constant for dephosphorylation, was indistinguishable from zero and could in fact be removed from Eq. 12 with no change to the fit. This is interesting, because previous direct measurements of the rate constant for dephosphorylation in the absence of $K^+$ but in the presence of $Mg^{2+}$ have yielded values in the range 2–7 $s^{-1}$ (17–19). Therefore, this result suggests that $Mg^{2+}$ may also have an allosteric effect in accelerating the rate of dephosphorylation. However, this possibility should be investigated by more direct measurements than those reported here. An allosteric effect of $Mg^{2+}$ on $k_3$ hasn't been included in Eq. 12. This could be done, but with the number of fitted parameters already included in the equation, a significantly better fit to the experimental data would not be obtained. The values of the other parameters obtained from the fit were $k_4^{min} = 13(\pm 4)s^{-1}$, $k_4^{max} = 74(\pm 10)s^{-1}$ and $K_F = 1.3\ (\pm\ 0.8) \times 10^3\ M^{-1}$. The value of $K_F$ corresponds to a dissociation constant of $Mg^{2+}$ with the E2ATP conformation of the protein of 0.8 ($\pm$ 0.5) mM. In comparison with the $E1ATP(Na^+)_3$ conformation, this represents an order of magnitude weaker binding of $Mg^{2+}$. It is interesting that this parallels a much weaker binding of ATP itself to the E2 conformation relative to the E1 conformation (26).

The value of $k_4^{max}$ derived from the fitting of 74 $s^{-1}$ is consistent with the values in the range 65–90 $s^{-1}$ (21–23) previously found for the E2 $\rightarrow$ $E1(Na^+)_3$ transition in the presence of saturating concentrations of $Mg^{2+}$ and ATP for $Na^+$,$K^+$-ATPase from pig and rabbit kidney. The lower value of $k_4^{min}$, the rate constant for the same transition but in the absence of $Mg^{2+}$, of 13 $s^{-1}$ is in accordance with the idea that $Mg^{2+}$ has an allosteric effect similar to ATP in accelerating this reaction. One needs to keep in mind, however, that although the fit shown in Fig. 3 is consistent with the data obtained for the fast phase, there are many more rate constants and equilibrium constants affecting the relaxation of the slow phase. This makes it difficult to give precise estimates of the parameters in the fitting model. For this reason, as in the case of the dephosphorylation reaction, the effect of $Mg^{2+}$ on the E2 $\rightarrow$ $E1(Na^+)_3$ transition should be investigated by more direct means, e.g., a direct analysis of the effect of $Mg^{2+}$ on the time course of the E2 $\rightarrow$ $E1(Na^+)_3$ reaction alone.

## DISCUSSION

The kinetics of $Na^+$- and $Mg^{2+}$-dependent reactions of the $Na^+,K^+$-ATPase have been investigated via the stopped-flow technique by mixing enzyme-containing membrane fragments fluorescently labeled with the probe RH421 with ATP at varying $Mg^{2+}$ concentrations. As in the case of previous stopped-flow studies using the same technique (10–12,21,22), two kinetic phases were observed, both associated with a fluorescence increase. The faster phase is attributed to the phosphorylation of the enzyme and its conversion to the E2MgP state. The slower phase is attributed to a subsequent relaxation of the dephosphorylation/rephosphorylation (via ATP) equilibrium and build-up of some enzyme in the E2Mg state.

It was found that both phases showed similar roughly hyperbolic increases in their observed rate constants to saturating values, but the $k_{obs}$ of the fast phase saturated at a lower $Mg^{2+}$ concentration than that of the slow phase. The $Mg^{2+}$ concentration dependence of the fast phase can be explained by $Mg^{2+}$ stimulation of the enzyme's phosphorylation by acting as a cofactor of ATP. This phase involves the direct phosphorylation of enzyme in the $E1Mg(Na^+)_3$ state by ATP. The slow phase also involves phosphorylation by ATP, but after the enzyme has proceeded once around its enzymatic cycle, i.e., after dephosphorylation and a conformational change back to the initial $E1Mg(Na^+)_3$ state. Since the slow phase also involves enzyme phosphorylation, the $Mg^{2+}$ concentration dependence of its $k_{obs}$ can also partly be explained by $Mg^{2+}$ stimulation of ATP phosphorylation. However, the fact that the slow phase saturates at a higher $Mg^{2+}$ concentration than the fast phase implies that this is not the only effect. The concentration dependence of the slow phase could be explained by an additional stimulation by $Mg^{2+}$ of the $E2ATP \rightarrow E1ATP(Na^+)_3$ reaction.

From crystal structures (32,33) of the related P-type ATPase, the sarcoplasmic reticulum $Ca^{2+}$-ATPase, it is known that $Mg^{2+}$ binds to the enzyme in a complex with a nucleotide (i.e., ATP under physiological conditions but its inert analog AMPPCP in crystals). To gain an insight into how $Mg^{2+}$ is held in place within the enzyme, it is interesting to compare the $Mg^{2+}$ $K_d$ determined here with the $K_d$ of $Mg^{2+}$ with ATP in free solution. We have recently determined this using isothermal titration calorimetry, under the same buffer conditions as used here for the stopped-flow measurements, to be 0.071 (± 0.003) mM (4). This is indistinguishable from the value of $K_d$ determined here in the presence of the enzyme, i.e., 0.069 (± 0.010) mM. This implies that although $Mg^{2+}$ carries out an important function in the enzyme's mechanism in allowing phosphoryl transfer, the enzyme environment of the E1 state has no effect on the strength of complexation of $Mg^{2+}$ by ATP. The enzyme does have to provide space within its structure so that $Mg^{2+}$ can access ATP, but it is the ATP, not the enzyme, that dominates in holding the $Mg^{2+}$ ion in place. This could explain why no crystal structure of an $E1Mg^{2+}$ state of a P-type ATPase has ever been determined despite success with many other states around the enzymatic cycle. Faller (34) recently reported a weak dissociation constant of $Mg^{2+}$ to the E2 form of the $Na^+,K^+$-ATPase of 2.5 mM. He attributed $Mg^{2+}$ binding alone to an ''induced-fit'' mechanism, because, as shown in crystal structures of the $Ca^{2+}$-ATPase, the protein residues that interact with the $Mg^{2+}$ ions are more than twice as far apart in the $Ca_2E1$ state (2) as in the E2 $P_i$ state (35). Therefore, in an $Na_3$ E1 state, one might expect an even weaker binding of $Mg^{2+}$ to the enzyme in the absence of ATP, i.e., $K_d > 2.5$ mM, but definitely much greater than the $K_d$ determined here for the E1ATP complex of 0.069 (± 0.010) mM. Schneeberger and Apell (29) reported an apparent $K_d$ of $Mg^{2+}$ to the E1 state of ~30 mM in the presence of 50 mM NaCl, but this was attributed to $Mg^{2+}$ binding to the $Na^+$ transport sites, not the site within the enzyme where it coordinates with ATP. Aspartate residues of the protein may be in relatively close proximity to the $Mg^{2+}$ required for phosphorylation, as suggested by Patchornik et al. (3), but it seems that their importance for the strength of binding of $Mg^{2+}$ is far outweighed by the phosphates of ATP. It needs to be pointed out, however, that the above argument does not rule out significant contributions of the enzyme toward the strength of $Mg^{2+}$ binding in other conformations of the enzyme cycle. It also needs to be made clear that the results described here only refer to the $Mg^{2+}$ ion necessary for phosphorylation, which acts as a cofactor of ATP. In crystals containing $Mg^{2+}$, ADP and the phosphate analog $AlF_4^-$ (36), which represents an E1 ~PADP transition state, a second $Mg^{2+}$ ion was found between the $\alpha$- and $\beta$-phosphates of ADP. This second $Mg^{2+}$ was, however, not present in the complex of the enzyme with AMPPCP, which is the more relevant state for this study.

## APPENDIX: SIMULATIONS

Computer simulations of the time course of fluorescence changes experimentally observed via stopped flow were performed using the program Berkeley Madonna 8.0 (University of California, Berkeley) via the variable-step-size Rosenbrock integration method. Based on reaction scheme A–C, the differential rate equations describing the changes in the concentrations of all the enzyme intermediates are

$$\frac{d\left[\mathrm{E1MgATP}\left(\mathrm{Na}^+\right)_3\right]}{dt} = -k_1\left[\mathrm{E1MgATP}\left(\mathrm{Na}^+\right)_3\right] \quad \text{(A1)}$$

$$\frac{d\left[\mathrm{E2MgP}\left(\mathrm{Na}^+\right)_3\right]}{dt} = k_1\left[\mathrm{E1MgATP}\left(\mathrm{Na}^+\right)_3\right] - k_2\left[\mathrm{E2MgP}\left(\mathrm{Na}^+\right)_3\right] + k_{-2}[\mathrm{E2MgP}] \quad \text{(A2)}$$

$$\frac{d[\mathrm{E2MgP}]}{dt} = k_2\left[\mathrm{E2MgP}\left(\mathrm{Na}^+\right)_3\right] - k_{-2}[\mathrm{E2MgP}] - k_3[\mathrm{E2MgP}] + k_{-3}[\mathrm{E2Mg}] \quad \text{(A3)}$$

$$\frac{d[\mathrm{E2Mg}]}{dt} = k_3[\mathrm{E2MgP}] - k_{-3}[\mathrm{E2Mg}]. \qquad \text{(A4)}$$

The total fluorescence, $F$, is due to contributions from fluorescence levels, $f$, of the probe associated with each of the enzyme conformational states. Because the fluorescence increases after mixing with ATP and the enzyme starts in the E1MgATP$(Na^+)_3$ state, we have defined the fluorescence level of this state to be zero. Because the major changes in fluorescence are thought to involve the binding or release of ions (14,20,27), the fluorescence level of the E1MgP$(Na^+)_3$ has also been taken to be zero. $F$ is then given by

$$F = f_{\mathrm{E2MgP}}[\mathrm{E2MgP}] + f_{\mathrm{E2Mg}}[\mathrm{E2Mg}]. \qquad \text{(A5)}$$

Numerical integration of Eqs. A1–A4 and calculation of $F$ using Eq. A5 yields a biexponential fluorescence transient with both phases associated with a fluorescence increase (as experimentally observed) using any values of $f_{\mathrm{E2MgP}}$ and $f_{\mathrm{E2Mg}}$ greater than zero. Based on the experimental results obtained, at saturating $Mg^{2+}$ concentrations, the values of $k_1$, $k_3$, and $k_{-3}$ used were 237 $s^{-1}$, 5 $s^{-1}$, and 63 $s^{-1}$, respectively. The values of $k_2$ and $k_{-2}$ for $Na^+$ release and binding to the E2MgP state were both chosen to have values of 1000 $s^{-1}$ (37).

The authors thank Prof. Helge Rasmussen, Royal North Shore Hospital, Sydney, for financial assistance supporting enzyme transport. R.J.C. acknowledges with gratitude financial support from the Australian Research Council/National Health and Medical Research Council-funded Research Network "Fluorescence Applications in Biotechnology and Life Sciences" (RN0460002) and the Department of Chemistry, Ben-Gurion University of the Negev, for a Dozor Visiting Fellowship.

## REFERENCES

1. Voet, D., and J. G. Voet. 1995. Biochemistry, 2nd ed. Wiley, New York.
2. Toyoshima, C., M. Nakasako, H. Nomura, and H. Ogawa. 2000. Crystal structure of the calcium pump of sarcoplasmic reticulum at 2.6 Å resolution. *Nature*. 405:647–655.
3. Patchornik, G., K. Munson, R. Goldshleger, A. Shainskaya, G. Sachs, et al. 2002. The ATP-$Mg^{2+}$ binding site and cytoplasmic domain interactions of $Na^+$,$K^+$-ATPase investigated with $Fe^{2+}$-catalyzed oxidative cleavage and molecular modelling. *Biochemistry*. 41:11740–11749.
4. Pilotelle-Bunner, A., J. M. Matthews, F. Cornelius, H.-J. Apell, P. Sebban, et al. 2008. ATP binding equilibria of the $Na^+$,$K^+$-ATPase. *Biochemistry*. 47:13103–13114.
5. Skou, J. C., and M. Esmann. 1988. Preparation of membrane $Na^+$,$K^+$-ATPase from rectal glands of *Squalus acanthias*. *Methods Enzymol*. 156:43–46.
6. Ottolenghi, P. 1975. The reversible delipidation of a solubilized sodium-plus-potassium ion-dependent adenosine triphosphatase. *Biochem. J*. 151:61–66.
7. Peterson, G. L. 1977. A simplification of the protein assay method of Lowry et al. which is more generally applicable. *Anal. Biochem*. 83:346–356.
8. Lowry, O. H., N. J. Rosebrough, A. L. Farr, and R. J. Randall. 1951. Protein measurement with the Folin phenol reagent. *J. Biol. Chem*. 193:265–275.
9. Jørgensen, P. L., and J. P. Andersen. 1988. Structural basis for $E_1$-$E_2$ conformational transitions in Na,K-pump and Ca-pump proteins. *J. Membr. Biol*. 103:95–120.
10. Kane, D. J., K. Fendler, E. Grell, E. Bamberg, K. Taniguchi, et al. 1997. Stopped-flow kinetic investigations of conformational changes of pig kidney $Na^+$,$K^+$-ATPase. *Biochemistry*. 36:13406–13420.
11. Cornelius, F. 1999. Rate determination in phosphorylation of shark rectal Na,K-ATPase by ATP: temperature sensitivity and effects of ADP. *Biophys. J*. 77:934–942.
12. Clarke, R. J., D. J. Kane, H.-J. Apell, M. Roudna, and E. Bamberg. 1998. Kinetics of the $Na^+$-dependent conformational changes of rabbit kidney $Na^+$,$K^+$-ATPase. *Biophys. J*. 75:1340–1353.
13. Pratap, P. R., and J. D. Robinson. 1993. Rapid kinetic analyses of the $Na^+/K^+$-ATPase distinguish among different criteria for conformational change. *Biochim. Biophys. Acta*. 1151:89–98.
14. Stürmer, W., R. Bühler, H.-J. Apell, and P. Läuger. 1991. Charge translocation by the Na,K-pump. II. Ion binding and release at the extracellular face. *J. Membr. Biol*. 121:163–176.
15. Mårdh, S., and Ö. Zetterqvist. 1974. Phosphorylation and dephosphorylation reactions of bovine brain ($Na^+$-$K^+$)-stimulated ATP phosphohydrolase studied by a rapid-mixing technique. *Biochim. Biophys. Acta*. 350:473–483.
16. Hobbs, A., R. W. Albers, and J. P. Froehlich. 1988. Complex time dependence of phosphoenzyme formation and decomposition in electroplax Na,K-ATPase. *In* The $Na^+$,$K^+$-Pump, Part A: Molecular Aspects. J. C. Skou, J. G. Nørby, A. B. Maunsbach, and M. Esmann, editors. Alan R. Liss, New York. 307–314.
17. Campos, M., and L. Beaugé. 1992. Effects of magnesium and ATP on pre-steady-state phosphorylation kinetics of the $Na^+$,$K^+$-ATPase. *Biochim. Biophys. Acta*. 1105:51–60.
18. Hobbs, A. S., R. W. Albers, and J. P. Froehlich. 1980. Potassium-induced changes in phosphorylation and dephosphorylation of ($Na^+$ + $K^+$)-ATPase observed in the transient state. *J. Biol. Chem*. 255:3395–3402.
19. Kane, D. J., E. Grell, E. Bamberg, and R. J. Clarke. 1998. Dephosphorylation kinetics of pig kidney $Na^+$,$K^+$-ATPase. *Biochemistry*. 37:4581–4591.
20. Apell, H.-J., M. Roudna, J. E. T. Corrie, and D. R. Trentham. 1996. Kinetics of the phosphorylation of Na,K-ATPase by inorganic phosphate detected by a fluorescence method. *Biochemistry*. 35:10922–10930.
21. Clarke, R. J., and D. J. Kane. 2007. Two gears of pumping by the sodium pump. *Biophys. J*. 93:4187–4196.
22. Lüpfert, C., E. Grell, V. Pintschovius, H.-J. Apell, F. Cornelius, et al. 2001. Rate limitation of the $Na^+$,$K^+$-ATPase pump cycle. *Biophys. J*. 81:2069–2081.
23. Humphrey, P. A., C. Lüpfert, H.-J. Apell, F. Cornelius, and R. J. Clarke. 2002. Mechanism of the rate-determining step of the $Na^+$,$K^+$-ATPase pump cycle. *Biochemistry*. 41:9496–9507.
24. Segel, I. H. 1975. Enzyme Kinetics: Behaviour and Analysis of Rapid Equilibrium and Steady-State Enzyme Systems. Wiley, New York.
25. Kong, B. Y., and R. J. Clarke. 2004. Identification of potential regulatory sites of the $Na^+$,$K^+$-ATPase by kinetic analysis. *Biochemistry*. 43:2241–2250.
26. Clarke, R. J., H.-J. Apell, and B. Y. Kong. 2007. Allosteric effect of ATP on $Na^+$,$K^+$-ATPase conformational kinetics. *Biochemistry*. 46:7034–7044.
27. Klodos, I. 1994. Partial reactions in $Na^+/K^+$- and $H^+/K^+$-ATPase studied with voltage-sensitive fluorescent dyes. *In* The Sodium Pump: Structure Mechanism, Hormonal Control and Its Role in Disease. E. Bamberg, and W. Schoner, editors. Steinkopff Verlag, Darmstadt, Germany. 517–528.
28. Schneeberger, A., and H.-J. Apell. 1999. Ion selectivity of the cytoplasmic binding sites of the Na,K-ATPase: I. Sodium binding is associated with a conformational rearrangement. *J. Membr. Biol*. 168:221–228.
29. Scheeberger, A., and H.-J. Apell. 2001. Ion selectivity of the cytoplasmic binding sites of the Na,K-ATPase. II. Competition of various cations. *J. Membr. Biol*. 179:263–273.
30. Grisham, C. M., and A. S. Mildvan. 1974. Magnetic resonance and kinetic studies of the mechanism of sodium and potassium ion-activated adenosine triphosphatase. *J. Biol. Chem*. 249:3187–3197.
31. Post, R. L., C. Hegyvary, and S. Kume. 1972. Activation by adenosine triphosphate in the phosphorylation kinetics of sodium and

potassium ion transport adenosine triphosphatase. *J. Biol. Chem.* 247:6530–6540.

32. Olesen, C., M. Picard, A. M.-L. Winther, C. Gyrup, J. P. Morth, et al. 2007. The structural basis of calcium transport by the calcium pump. *Nature*. 450:1036–1046.
33. Toyoshima, C. 2008. Structural aspects of ion pumping by $Ca^{2+}$-ATPase of sarcoplasmic reticulum. *Arch. Biochem. Biophys*. 476:3–11.
34. Faller, L. D. 2008. Mechanistic studies of sodium pump. *Arch. Biochem. Biophys*. 476:12–21.
35. Toyoshima, C., H. Nomura, and T. Tsuda. 2004. Lumenal gating mechanism revealed in calcium pump crystal structures with phosphate analogues. *Nature*. 432:361–368.
36. Sørensen, T. L.-M., J. V. Møller, and P. Nissen. 2004. Phosphoryl transfer and calcium ion occlusion in the calcium pump. *Science*. 304:1672–1675.
37. Holmgren, M., J. Wagg, F. Bezanilla, R. F. Rakowski, P. De Weer, et al. 2000. Three distinct and sequential steps in the release of sodium ions by the $Na^+,K^+$-ATPase. *Nature*. 403:898–901.